Photochemical & Photobiological Sciences

RSC Publishing

PAPER

# Step-wise addition of disulfide bridge in firefly luciferase controls color shift through a flexible loop: a thermodynamic perspective†

Cite this: *Photochem. Photobiol. Sci.*, 2013, **12**, 298

Mahboobeh Nazari,[a] Saman Hosseinkhani*[a] and Leila Hassani[b]

Received 9th May 2012,
Accepted 30th August 2012

DOI: 10.1039/c2pp25140j

**www.rsc.org/pps**

Multi-color bioluminescence is developed using the introduction of single/double disulfide bridges in firefly luciferase. The bioluminescence reaction, which uses luciferin, $Mg^{2+}$-ATP and molecular oxygen to yield an electronically excited oxyluciferin, is carried out by the luciferase and emits visible light. The bioluminescence color of firefly luciferases is determined by the luciferase sequence and assay conditions. It has been proposed that the stability of a protein may increase through the introduction of a disulfide bridge that decreases the configurational entropy of unfolding. Single and double disulfide bridges are introduced into *Photinus pyralis* firefly luciferase to make separate mutant enzymes with a single/double bridge ($C^{81}$–$A^{105}C$, $L^{306}C$–$L^{309}C$, $P^{451}C$–$V^{469}C$; $C^{81}$–$A^{105}C/P^{451}C$–$V^{469}C$, and $A^{296}C$–$A^{326}C/P^{451}C$–$V^{469}C$). By introduction of disulfide bridges using site-directed mutagenesis in *Photinus pyralis* luciferase the color of emitted light was changed to red or kept in different extents. The bioluminescence color shift occurred with displacement of a critical loop in the luciferase structure without any change in green emitter mutants. Thermodynamic analysis revealed that among mutants, $L^{306}C$–$L^{309}C$ shows a remarkable stability against urea denaturation and also a considerable increase in kinetic stability and a clear shift in bioluminescence spectra towards red.

## Introduction

Luciferases are made by a wide variety of phyla, including bioluminescent species such as beetles, fireflies, bacteria, and marine coelenterates and dinoflagellates.[1–6] Firefly luciferase catalyzes the oxidation of luciferin in the presence of ATP, $Mg^{2+}$, and molecular oxygen.[7] This enzyme efficiently converts chemical energy into light with high quantum yield.[8,9] The most widely used luciferase reporter gene is that of the North American firefly, *Photinus pyralis*. Wild-type, *P. pyralis* luciferase is thermolabile, with an *in vitro* half-life for activity of the order of 2–3 min at 37 °C. Although firefly luciferase has been used in different bioluminescence-based technologies, several hindering factors, such as low stability of the enzyme either *in vivo* or *in vitro*, rapid loss of activity even at room temperature, high $K_m$ for the ATP, pH intolerance (a large red-shift in its bioluminescence spectrum at low pH), and low relative specific activity limited its applications. So, several intensive efforts have been made to develop a thermostable enzyme with improved properties using different technologies, such as site-directed mutagenesis,[10–15] gene chimerization[16] and random mutagenesis.[17] We have recently reported the introduction of a disulfide bond in firefly luciferase, which was accompanied by an increase of thermostability, red shift color and decrease of pH-sensitivity.[18,19]

There is considerable interest in measuring the conformational stability because globular proteins are only biologically active when they are folded.[20] It has been clear for many years that the conformational stability of globular proteins is remarkably low, generally between 5 and 15 kcal $mol^{-1}$.[21,22] However, there has been uncertainty in how accurately the conformational stability can be measured. The two methods most often used to estimate the conformational stability are differential scanning calorimetry (DSC)[23–25] and solvent denaturation studies using urea and guanidine hydrochloride (GdnHC1).[26,27] Both methods require an extrapolation of the results from the conditions used to promote unfolding to physiological conditions.[26–29]

Solvent denaturation experiments yield $\Delta G^{\circ}$ as a function of denaturant concentration. The comparison of the values obtained from a wild-type and a mutant protein constitutes a common method to obtain information about the role of certain interactions in the structure and stability of the protein.[30,31]

[a]*Department of Biochemistry, Faculty of Biological Sciences, Tarbiat Modares University, Tehran, Iran. E-mail: saman_h@modares.ac.ir; Fax: +(98)-21-82884484; Tel: +(98)-21-82884407*

[b]*Department of Biological Sciences, Institute for Advanced Studies in Basic Sciences (IASBS), Zanjan 45195–1159, Iran*

†Electronic supplementary information (ESI) available. See DOI: 10.1039/c2pp25140j

Luciferase stability and color shift are correlated among the mutants of firefly luciferases studied in this paper. Indeed, in order to elucidate the mechanisms of the bioluminescence color change, extensive studies were carried out and several mechanisms have been proposed.[32] Multiple sequence alignment of the primary structure of *Phrixothrix hirtus*, the only natural red light emitter, showed a missing $Arg^{353}$ in a flexible loop in green emitter firefly luciferases. Accordingly, site directed mutagenesis was used for the insertion of Arg in the corresponding position in a flexible loop of firefly (*Lampyris turkestanicus*) luciferase[33,34] and it was shown that $Arg^{353}$ plays a critical role in the bioluminescence color and thermostability.[10] A similar study on the North American firefly luciferase *Photinus pyralis* indicated that the presence of positive charges on the same loop has significant effects on the emitted light, shifting from green to red.[35,36]

In this study, our main goal was the introduction of two disulfide bridges into firefly luciferase based on previous results and the investigation of the role of those bridges on the structure and function of firefly luciferase.[18,19] Therefore, site-directed mutagenesis was used to introduce new cysteine residues suitable for disulfide bridge formation ($A^{296}C$–$A^{326}C$/$P^{451}C$–$V^{469}C$, and $C^{81}$–$A^{105}C$/$P^{451}C$–$V^{469}C$). Then, we have characterized the structural stability of firefly luciferase (*P. pyralis*) and its mutants ($C^{81}$–$A^{105}C$, $L^{306}C$–$L^{309}C$, $P^{451}C$–$V^{469}C$, $A^{296}C$–$A^{326}C$/$P^{451}C$–$V^{469}C$, and $C^{81}$–$A^{105}C$/$P^{451}C$–$V^{469}C$) by equilibrium unfolding studies, using urea as a protein denaturant. Analysis of the unfolding process of the native and mutant luciferases *via* fluorescence spectroscopy provides a measure of structural stability. Our data show that introduction of a disulfide bridge plays a significant role in the stability and bioluminescence color of *P. pyralis* luciferase.

**Abbreviations**: in this paper, we designate genetic derivatives of *P. pyralis* firefly luciferase. Replacements are abbreviated, using the single-letter code for amino acids; in this manner, replacement of leucine-306 with cysteine is abbreviated $L^{306}C$. Multiple replacements are listed separated by – for a disulfide bond, *e.g.*, $Leu^{306}C$–$L^{309}C$. Double disulfide bonds are separated by diagonal slashes, *e.g.*, $C^{81}$–$A^{105}C$/$P^{451}C$–$V^{469}C$.

## Experimental procedures

### Materials

The following reagents and kits were used. Isopropyl-β-D-thiogalactopyranoside (IPTG), kanamycin, ATP (Roche); D-luciferin potassium salt (Synchem); ANS, 8-anilino-naphthalene-1-sulfonic acid and DTNB (5,5′-dithio-bis-(2-nitrobenzoic acid)) (Merk, Germany); Pfu polymerase, plasmid extraction kit, gel purification kit, PCR purification (Bioneer CO., South Korea), Expand DNA polymerase (Roche), Ni-NTA Sepharose (QIAGEN Inc.), and pET28a vector (Novagen).

Please see ESI for the design and construction of disulfide bridges (Table S1†).

### Site directed mutagenesis

For the preparation of the mutants with two disulfide bridges, the Quick-change site-directed mutagenesis protocol was used with application of a mega-primer. F primer $P^{451}C$ and R primer $V^{469}C$ were used for generation of the megaprimer. Single disulfide mutant pET-28a containing $C^{81}$–$A^{105}C$ and $A^{296}C$–$A^{326}C$ was used as a template by Pfu polymerase under the following conditions: initial denaturation at 94 °C for 5 min, a 35 cycle (94 °C for 1 min, 55 °C for 1 min, and 72 °C for 20 s), and a final extension for 1 min at 72 °C. The synthetic megaprimer was used in a new PCR reaction under the following conditions: initial denaturation at 95 °C for 3 min, a 22 cycle (95 °C for 1 min, 68 °C for 13 min), and a final extension for 10 min at 68 °C. After amplification, plasmids containing staggered nicks were generated. Subsequently, primary PCR products were purified using a clean-up kit to remove the redundant primers. The products were treated with Dpn1 in order to digest native parental plasmids, and used directly to transform into competent cells *E. coli* XL1-Blue by electroporation.

Protein expression and purification, thiol titration, measurement of bioluminescence emission spectra, kinetic properties, thermal inactivation and thermal stability were carried out as previously described (also see ESI†).[18,19,37]

### Fluorescent measurements

The purified luciferases were dialyzed in dialysis buffer containing 50 mM Tris-HCl, 1% glycerol, 1 mM EDTA, and 50 mM NaCl (pH 7.8) at 4 °C. Fluorescence studies were carried out on a Cary-Eclipse luminescence spectrophotometer (Varian). Intrinsic fluorescence was determined using 25 μg $mL^{-1}$ protein and an excitation wavelength of 295 nm. Emission spectra were recorded between 300 and 400 nm.[38] Extrinsic fluorescence studies were carried out with 8-anilino-1-naphthalenesulfonic acid (ANS) as a fluorescence probe. Measurements were taken on the same spectrofluorimeter that was used for intrinsic fluorescence studies. All experiments were carried out at 25 °C. The final concentration of the ANS in the enzyme solutions was 30 μM, and the molar ratio of protein to ANS was 1 : 50. The ANS emission was scanned between 400 and 650 nm with an excitation wavelength of 350 nm.[39] Data reported represent the average of three spectra.

### Data analysis

Denaturation curves were obtained by plotting the fluorescence intensities at 330 nm, the emission maximum for the protein, *versus* the denaturant molarity. Data presented in the urea denaturation curve was analyzed using the linear extrapolation method as described by Pace[27], Santoro and Bolen,[28] and Pace *et al.*[40] The analysis was based on the assumption of a two-state mechanism of unfolding,

$$N \leftrightarrow D \quad (1)$$

According to the two states mechanism, the native and denaturated states are present in significant concentrations in

the transition region. Therefore, if $f_N$ and $f_D$ represent the fractions of protein present in the folded and unfolded conformations, respectively, then $f_N + f_D = 1$. The observed value of fluorescence intensity $Y$ at any point will be $Y_N f_N + Y_D f_D$, where $Y_N$ and $Y_D$ represent the values of $Y$ characteristic of the native and denaturated states, respectively. Combining these equations,

$$f_D = (Y - Y_N)/(Y_D - Y_N) \text{ and } f_N = (Y_D - Y)/(Y_D - Y_N)$$

Therefore, the equilibrium constant $K$ and $\Delta G_U$, the free energy of unfolding, were calculated using

$$K = f_D/f_N = (Y - Y_N)/(Y_D - Y) \quad (2)$$

$$\Delta G_U = -RT\ln K = -RT\ln((Y - Y_N)/(Y_D - Y)) \quad (3)$$

where $R$ is the gas constant (8.3143 J $deg^{-1}$ $mol^{-1}$) and $T$ is the absolute temperature.

It is assumed that $\Delta G_U$ has a linear dependence on the concentration of denaturant (D)

$$\Delta G_U = \Delta G(H_2O) - m(D) \quad (4)$$

where $m$ is a measure of the dependence of $\Delta G_U$ on the denaturant concentration and is given by the slope of the line describing the dependence of $\Delta G_U$ on (D) and $\Delta G(H_2O)$ corresponds to the free energy of unfolding extrapolated to zero denaturant concentration.

The denaturant concentration at which the protein is half-unfolded (when $\Delta G_U = 0$) is given by $D_{1/2}$ and from eqn (4),

$$D_{1/2} = \Delta G(H_2O)/m$$

### Activity measurements of luciferases in the presence of urea

Before activity measurement, 0.05 mg $mL^{-1}$ of native and mutant luciferases were incubated in different concentrations of urea (0–6 M) in 0.5 M intervals, for 20 min. Light emission of the samples were measured by a luminometer (Berthold Detection Systems, GmbH, Germany). The residual activities were plotted *versus* urea concentration.

### Bioinformatics study

*P. pyralis* firefly luciferase (Protein Data Bank (PDB) entry 1LCI) is used as the PDB template in the M4T Alignment Interface protein modeling server, by producing accurate alignments and models by minimizing the errors associated with the first two steps (template recognition and alignment), three-dimensional structural models of native and mutant luciferases were obtained.[41,42] The fit between the three-dimensional structures of models was evaluated with SWISS-PDB Viewer after iterative fitting. The network of hydrogen bonds in native and mutants were obtained using PIC[43] and the WHAT IF server.

## Results and discussion

### Construction, expression, and purification of the native and mutant luciferases

According to the results of the MODIP server and disulfide-by design, as previously described, the selected mutants were ($C^{81}$–$A^{105}C$, $L^{306}C$–$L^{309}C$, $P^{451}C$–$V^{469}C$, and $A^{296}C$–$A^{326}C$). Accordingly, two mutant luciferases with two disulfide bridges ($A^{296}C$–$A^{326}C/P^{451}C$–$V^{469}C$, and $C^{81}$–$A^{105}C/P^{451}C$–$V^{469}C$) were constructed and successfully expressed in *E. coli* (origami2). Wild type and all mutant luciferases were similar with respect to expression levels and yields of purification. The protein yields for wild-type and all mutants except $L^{306}C$–$L^{309}C$ were the same and it was 2–3 mg $mL^{-1}$ or 2–3 g $L^{-1}$, but for the $L^{306}C$–$L^{309}C$ mutant was 0.5 mg $mL^{-1}$ or 0.5 g $L^{-1}$. The purification of $His_6$-tagged fusion luciferases was also performed by affinity (Ni-NTA Sepharose) chromatography. The purified native and mutant luciferases had purities more than 95% on the basis of the analysis by SDS-PAGE in which luciferases were present as a band of 62 kDa. Upon addition of D-luciferin to purified luciferases, visible light was observed in the dark by the naked eye at pH 7.8. Disulfide formation was also indicated by the fact that the introduced Cys residues formed a disulfide bridge instead of remaining free thiol groups to react with DTNB (Ellman's reagent).[44]

### Bioluminescence emission spectra

The *in vitro* bioluminescence spectra of native and mutant enzymes were measured at pH 7.8, 25 °C and physiological conditions (pH 7.4; 37 °C). Among mutants, $P^{451}C$–$V^{469}C$ and $L^{306}C$–$L^{309}C$ mutants exhibit a single peak in the red region of the spectrum at pH 7.8. $A^{296}C$–$A^{326}C$ and $C^{81}$–$A^{105}C/P^{451}C$–$V^{469}C$ mutants display a bimodal spectrum with a maximum in the green region (561 nm) and a smaller shoulder (601 nm) in the red region. The native form and the $C^{81}$–$A^{105}C$ mutant exhibit a similar spectrum with only a peak in the green region (559 nm) and the $A^{296}C$–$A^{326}C/P^{451}C$–$V^{469}C$ mutant display a single peak at 576 nm (Fig. 1). Wild type and all mutants except $C^{81}$–$A^{105}C$ and $A^{296}C$–$A^{326}C$ showed the classic red shift[9,45] of bioluminescence spectra at elevated temperature and reduced pH (pH 7.4; 37 °C).

### Characterization of kinetic properties

Hanes plots were used to estimate the apparent $K_m$ values for luciferin ($LH_2$ $K_m$) and ATP (ATP $K_m$). The results (relative specific activity, optimum pH, and $K_m$ (for $LH_2$ and ATP)) are listed in Table 1. The $K_m$ values of $L^{306}C$–$L^{309}C$ for luciferin increased 2 times, for $P^{451}C$–$V^{469}C$, and $C^{81}$–$A^{105}C/P^{451}C$–$V^{469}C$ mutants increased 4 times, while that for $A^{296}C$–$A^{326}C$, $C^{81}$–$A^{105}C$, and $A^{296}C$–$A^{326}C/P^{451}C$–$V^{469}C$ were equal to the native form. The $K_m$ values of $C^{81}$–$A^{105}C$, and $A^{296}C$–$A^{326}C$ mutants for ATP decreased up to 85% and 70%, respectively, while that for $L^{306}C$–$L^{309}C$, $C^{81}$–$A^{105}C/P^{451}C$–$V^{469}C$, and $A^{296}C$–$A^{326}C/P^{451}C$–$V^{469}C$ mutants increased up to 2 times. The time of light decay was measured by injection of a 50 μL cocktail (2 mM luciferin, 4 mM ATP, and 10 mM $MgSO_4$ in 50 mM

 

Tris-HCl (pH 7.8)) to 50 μL of native and mutant purified enzymes (Fig. S5†). Subtle changes in optimum pH for mutant luciferases ($L^{306}C–L^{309}C$, $P^{451}C–V^{469}C$, and $A^{296}C–A^{326}C$), were also observed (Table 1) but for $C^{81}–A^{105}C/P^{451}C–V^{469}C$ and $C^{81}–A^{105}C$, $A^{296}C–A^{326}C/P^{451}C–V^{469}C$ mutant luciferases display an increase from 8 to 8.5 and 9, respectively.

### Effect of the mutations on the structure of the protein

Far-UV CD spectra, intrinsic fluorescence and ANS fluorescence spectra of the native and mutant forms of the enzyme are shown in Fig. 2 and 3, respectively. As shown, the intensity of the intrinsic fluorescence spectrum of the $L^{306}C–L^{309}C$ mutant reduces compared with the native protein. Also, the intensity of their far-UV CD spectrum is significantly decreased. This change occurs not only in the range of 190–200 nm with the positive CD signal but also at around 200–250 nm where it is negative. The observed changes in CD and fluorescence spectra implicate changes of secondary and tertiary structures of the enzyme with the mentioned mutations. As shown in Fig. 3B, ANS emission in the presence of mutant luciferases is increased and shifts to shorter wavelengths, indicating exposure of the hydrophobic groups to the solvent upon the mutation. Unlike the $L^{306}C–L^{309}C$ mutant, the hydrophobic groups of other mutants become more hidden.

As shown in Fig. 2 and 3, the changes occurring in the $P^{451}C–V^{469}C$ mutant are similar to the $C^{81}–A^{105}C$ mutant but the changes in the $C^{81}–A^{105}C$ mutant are significantly more than in the $P^{451}C–V^{469}C$ mutant.

In general, the spectroscopic results demonstrate dependence on the location of the introduced disulfide bond, both increasing and decreasing in observed Trp emissions, which

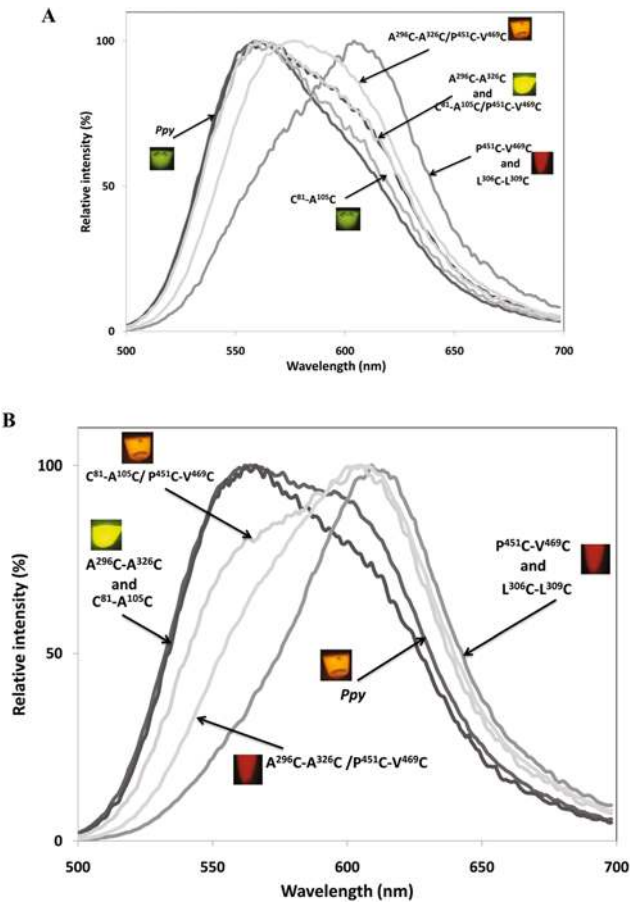


**Fig. 1** Normalized bioluminescence emission spectra of wild-type and mutant luciferases (A) at 25 °C, pH 8.0 and (B) at 37 °C, pH 7.4.

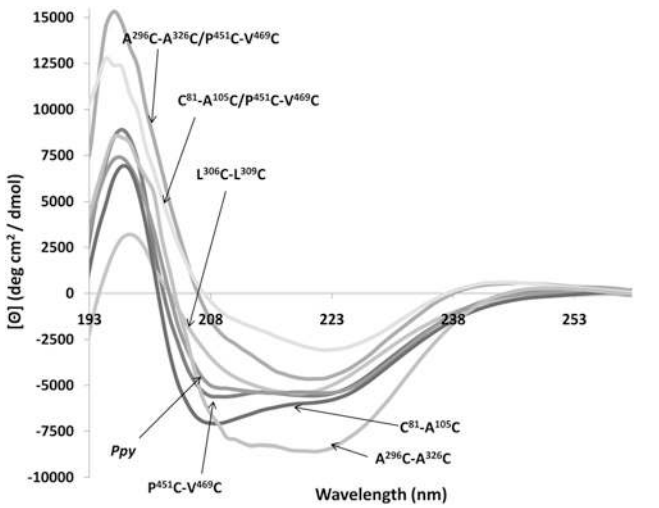


**Fig. 2** Far-UV CD spectra for the wild-type and mutant luciferases. The concentration of protein used for the far-UV CD spectrum (200–250 nm) was 0.2 mg $mL^{-1}$. Each enzyme was equilibrated in Tris-HCl buffer (0.05 M, pH 8.0) at 25 °C.

**Table 1** Kinetic properties of the wild-type and mutant luciferases

| Enzyme | Specific activity/($\times 10^{10}$) RLU $s^{-1}$ $mg^{-1}$ | Relative activity | $K_m$ [a] (μM) | | Optimum | |
|---|---|---|---|---|---|---|
| | | | ATP (μM) | $LH_2$ (μM) | Temperature[b] (°C) | pH[c] |
| *Ppy* | 2.72 | 100 | 110 | 8 | 25 | 8 |
| $C^{81}–A^{105}C$ | 5.7 | 208 | 100 | 10 | 35 | 9 |
| $L^{306}C–L^{309}C$ | 0.12 | 4 | 200 | 18 | 30 | 8 |
| $P^{451}C–V^{469}C$ | 1.4 | 51 | 120 | 40 | 25 | 8 |
| $A^{296}C–A^{326}C$ | 19.65 | 720 | 55 | 7 | 40 | 8 |
| $A^{296}C–A^{326}C/P^{451}C–V^{469}C$ | 1.185 | 43 | 180 | 45 | 30 | 9 |
| $C^{81}–A^{105}C/P^{451}C–V^{469}C$ | 0.65 | 32 | 200 | 11 | 30 | 8.5 |

[a] The error associated with the $K_m$ values falls within ±10% of the value. [b] See ESI Fig. S4.† [c] See ESI Fig. S3.†

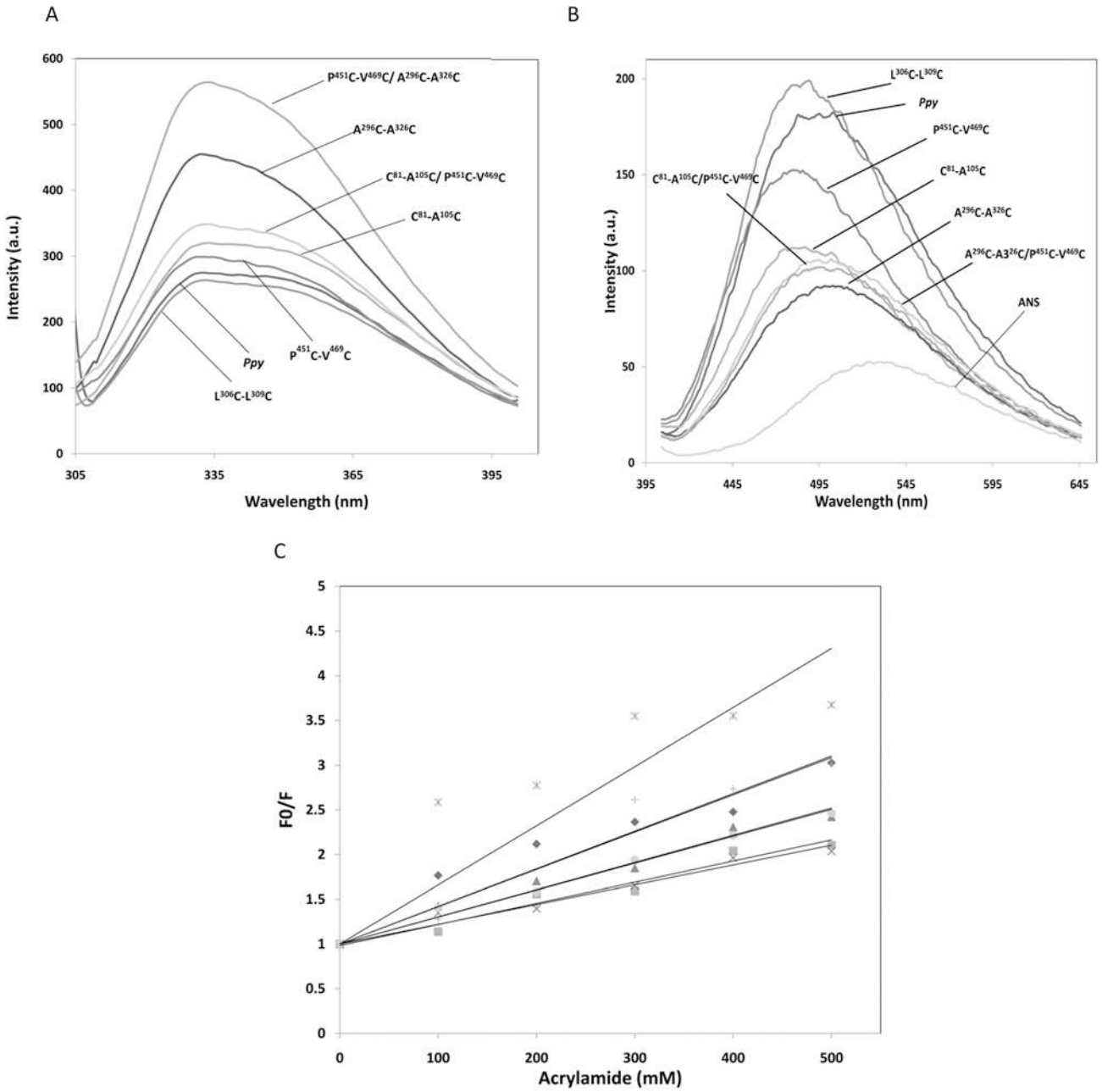


**Fig. 3** Comparison of intrinsic fluorescence (A) and ANS (B) in wild-type and mutant luciferases. Stern–Volmer plots of wild-type (◆) and mutant ($C^{81}$–$A^{105}C$ (■), $P^{451}C$–$V^{469}C$ (▲), $L^{306}C$–$L^{309}C$ (*), $A^{296}C$–$A^{326}C$ (×), $C^{81}$–$A^{105}C/P^{451}C$–$V^{469}C$ (●), and $A^{296}C$–$A^{326}C/P^{451}C$–$V^{469}C$ (+)), luciferases obtained by quenching with acrylamide (C). The excitation and emission wavelengths were 295 and 340 nm, respectively. The protein was dissolved in 0.05 M Tris-HCl buffer (pH 8.0), and the protein concentration was 30 mg $mL^{-1}$ in all samples.

show changes in the protein structure. As expected, decreases and increases in compactness of the structure are accompanied by exposure and hiding of the hydrophobic groups.

### Effect of the mutations on the chemical stability of the protein

*P. pyralis* luciferase has two tryptophan residues, $Trp^{417}$ and $Trp^{426}$; these Trp residues are located in a large N-terminal domain near the protein surface. To determine the spectroscopic contributions of the Trp residues, the conformational changes in mutants and native (*Ppy*) forms upon treatment with different concentrations of urea were evaluated by measuring the intrinsic fluorescence intensity. The effect of denaturant (urea) on the fluorescence emission properties of native (*P. pyralis*) and mutant firefly luciferases is shown in Fig. S6.† Intrinsic fluorescence intensity is reduced in *Ppy* and all mutants except for $L^{306}C$–$L^{309}C$ with a continuous increase in urea concentration. An increase in the fluorescence emission of the mutant $L^{306}C$–$L^{309}C$ was observed between 0.0–1.5 M urea.

 

Continuous reduction in the intensity of the spectra indicates that denaturant increase causes changes in the tertiary structure of the protein and exposure of excitable amino acids to a more polar environment.

The data obtained from fluorescence spectra was utilized to draw the denaturation curves, which were then analyzed to obtain $\Delta G_U$, using eqn (2)–(4). $\Delta G_U$ was plotted as a function of concentration of urea to obtain $D_{1/2}$ and $\Delta G(H_2O)$ (eqn (4)). The values of $D_{1/2}$ and $\Delta G(H_2O)$ of the native and mutant luciferases are shown in Table 2.

Fig. 4 shows $\Delta G_U$ as a function of denaturant concentration in native and mutant luciferases. The urea concentration at the mid-point of the unfolding transition was determined from Fig. 5A, B.

As is clear in Table 2, introduction of disulfide bonds in all mutant forms results in an increase in $\Delta G(H_2O)$ and $D_{1/2}$. The highest values of $D_{1/2}$ and $\Delta G(H_2O)$ were obtained for $L^{306}C$–$L^{309}C$.

The large $\Delta(\Delta G)$ of 7.16 kJ mol$^{-1}$ for the $L^{306}C$–$L^{309}C$ mutant indicates that the introduction of the disulfide bridge has a major stabilizing effect on the protein structure.

**Table 2** Chemical denaturation parameters measurement of wild-type and mutant luciferases. $D_{1/2}$, $\Delta G_{H2O}$ and $m$ values were obtained by linear extrapolation from a plot of $\Delta G_U$ as a function of urea concentration using eqn (4), as described in Materials and methods

| Sample | $\Delta G(H_2O)$ (kJ mol$^{-1}$) | $\Delta(\Delta G)$ (kJ mol$^{-1}$) | $D_{1/2}$ | $m$ value |
|---|---|---|---|---|
| *Ppy* | 2.54+ | — | 1.53 | 1.69 |
| $P^{451}C$–$V^{469}C$ | 4.36+ | 1.82 | 2.53 | 1.73 |
| $L^{306}C$–$L^{309}C$ | 9.70+ | 7.16 | 4.25 | 2.3 |
| $C^{81}$–$A^{105}C$ | 3.11+ | 0.57 | 2.15 | 1.44 |
| $C^{81}$–$A^{105}C/P^{451}C$–$V^{469}C$ | 4.8+ | 2.26 | 2.98 | 1.61 |
| $A^{296}C$–$A^{326}C/P^{451}C$–$V^{469}C$ | 3.27+ | 0.73 | 1.75 | 1.87 |

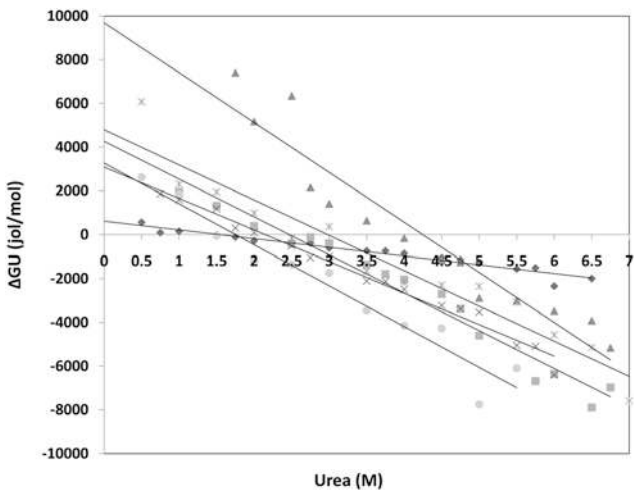


**Fig. 4** $\Delta G_U$ changes of in wild-type (◆) and mutant ($C^{81}$–$A^{105}C$ (×), $P^{451}C$–$V^{469}C$ (■), $L^{306}C$–$L^{309}C$ (▲), $C^{81}$–$A^{105}C/P^{451}C$–$V^{469}C$ (*), and $A^{296}C$–$A^{326}C/P^{451}C$–$V^{469}C$ (●)) luciferases in the presence of different concentrations of urea at 25 °C. $\Delta G_U$ were obtained as described in the experimental procedures.

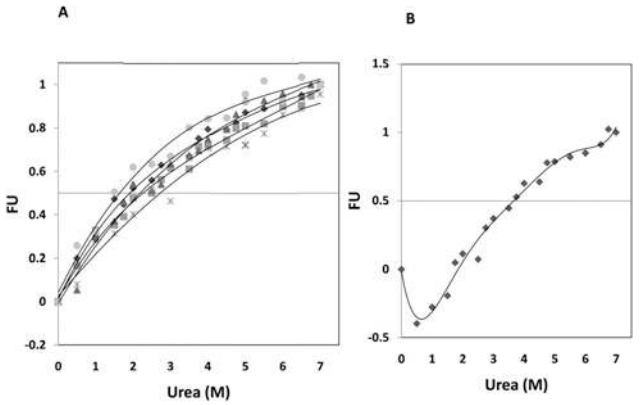


**Fig. 5** Urea concentrations at the mid-point of the unfolding transition (A), wild-type (◆) and mutant ($C^{81}$–$A^{105}C$ (■), $P^{451}C$–$V^{469}C$ (▲), $A^{296}C$–$A^{326}C/P^{451}C$–$V^{469}C$ (●), $C^{81}$–$A^{105}C/P^{451}C$–$V^{469}C$ (*)) and (B) $L^{306}C$–$L^{309}C$. Intrinsic fluorescence was determined using 25 μg mL$^{-1}$ protein and an excitation wavelength of 295 nm. Emission spectra were recorded between 300 and 400 nm.

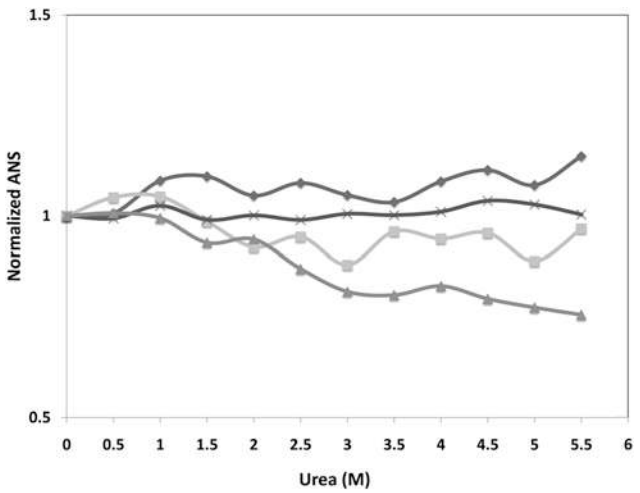


**Fig. 6** Fluorescence spectra of ANS ($\lambda_{max}$) plotted as a function of urea in wild-type (◆) and mutants ($C^{81}$–$A^{105}C$ (▲), $P^{451}C$–$V^{469}C$ (■), and $L^{306}C$–$L^{309}C$ (×)). Inset: ANS fluorescence spectra of wild-type and mutant luciferases at 6 M urea. The final concentration of the ANS in the enzyme solutions was 30 mM at 25 °C. The ANS emission was scanned between 400 and 650 nm with an excitation wavelength of 350 nm.

Moreover, the highest resistance against urea denaturation was observed for the $L^{306}C$–$L^{309}C$ mutant according to the accessibility of hydrophobic patches of the protein to ANS upon unfolding (Fig. 6).

## Residual activity

As shown in Fig. 7, residual activities of the native and mutant luciferases are decreased in the presence of urea in a concentration dependent manner. When urea concentrations were above 3 M, no residual activity could be detected. In addition, unlike the other samples, a slight increase of activity of the $L^{306}C$–$L^{309}C$ mutant was observed between 0.0–1.5 M urea. As noted, similar phenomena were observed in the intrinsic

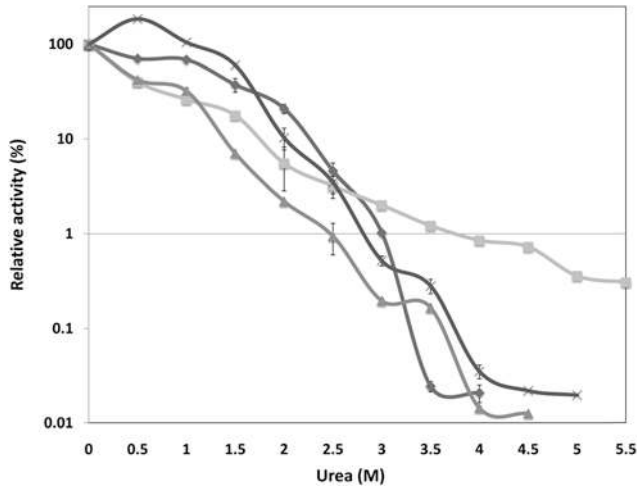


**Fig. 7** Activity measurements of wild-type (◆) and mutant ($C^{81}$–$A^{105}C$ (■), $P^{451}C$–$V^{469}C$ (▲), and $L^{306}C$–$L^{309}C$ (×)) in the presence of different urea concentrations (0, 0.5, 1, 1.5, 2, 2.5, 3, 3.5, 4, 4.5, 5, 5.5 and 6 M). The assays were conducted in Tris buffer at pH 8.00; in 25 °C. Results were in triplicate.

fluorescence as an increase in fluorescence intensity at low concentrations of urea was obtained. It seems there is a relation between residual activity and the tertiary structure of the $L^{306}C$–$L^{309}C$ mutant under weak denaturation conditions.

### Comparison of thermal stability of the native and mutant luciferases

The thermal stability of mutant luciferases was compared with native luciferase. The thermal inactivation experiments of the mutants $A^{296}C$–$A^{326}C$, $A^{296}C$–$A^{326}C/P^{451}C$–$V^{469}C$, $L^{306}C$–$L^{309}C$, $P^{451}C$–$V^{469}C$, $C^{81}$–$A^{105}C$, $P^{451}C$–$V^{469}C$, and $C^{81}$–$A^{105}C$ showed that their original activity remained at approximately 88%, 32%, 26%, 20%, 12% and 5% after incubation at 40 °C for 5 min, respectively, whereas the native enzyme lost nearly all of its activity (Fig. 8A). In addition to thermal inactivation studies, the thermal stability analysis of native and mutants enzymes at 32 °C showed that $L^{306}C$–$L^{309}C$, $A^{296}C/A^{326}C$, $P^{451}C$–$V^{469}C/A^{296}C$–$A^{326}C$, and $C^{81}$–$A^{105}C$ remained at 70%, 47%, 22%, and 22% of their original activities, respectively, while the remaining activity of the native enzyme was only 10% after 35 min (Fig. 8B).

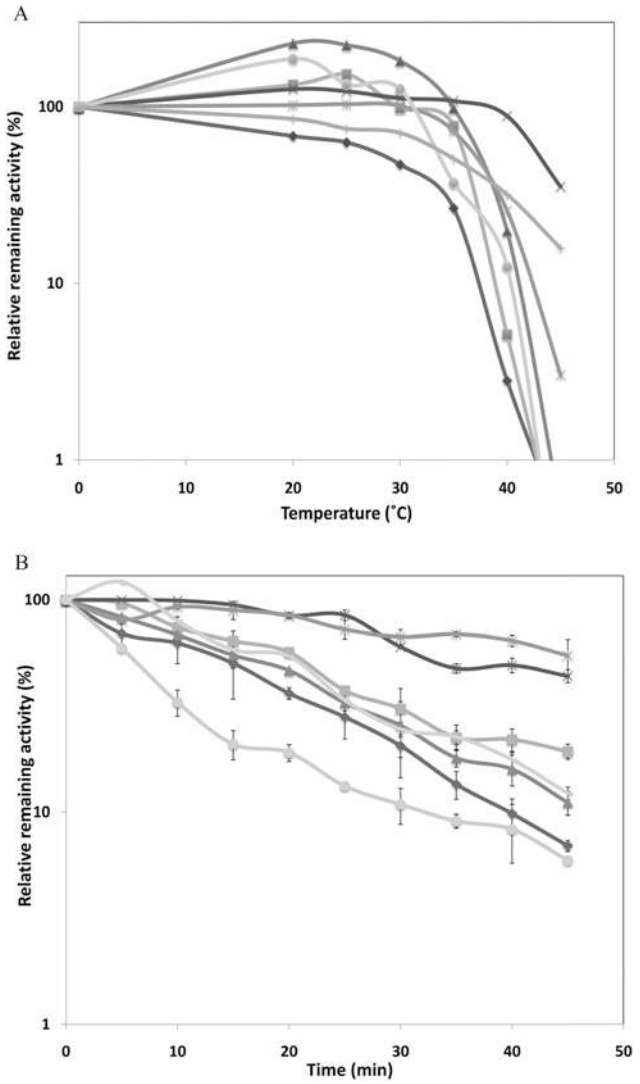


**Fig. 8** Comparison of thermal inactivation (A) and thermal stability (B) of wild-type (◆) and mutant ($C^{81}$–$A^{105}C$ (■), $P^{451}C$–$V^{469}C$ (▲), and $L^{306}C$–$L^{309}C$ (*), $A^{296}C$–$A^{326}C$ (×), $C^{81}$–$A^{105}C/P^{451}C$–$V^{469}C$ (●), and $A^{296}C$–$A^{326}C/P^{451}C$–$V^{469}C$ (–)), luciferases. The error associated with each point falls within 5% of the value. For further details, see Experimental procedures. $A^{296}C$–$A^{326}C$, $A^{296}C$–$A^{326}C/P^{451}C$–$V^{469}C$, $L^{306}C$–$L^{309}C$, $P^{451}C$–$V^{469}C$, $C^{81}$–$A^{105}C$, $P^{451}C$–$V^{469}C$, and $C^{81}$–$A^{105}C$ mutants kept approximately 88%, 32%, 26%, 20%, 12% and 5% of their original activity after incubation at 40 °C for 5 min, respectively.

### Bioinformatics study

The crystal structure of *P. pyralis* firefly luciferase was used as a template to elucidate the structure of the mutant luciferases. The location of the $L^{306}C$–$L^{309}C$ mutant is compared with the $A^{296}C$–$A^{326}C$ position (Fig. 9), which indicates loss of freedom in the connecting loop ($K^{303}$YDCSNCH$^{310}$) which may cause thermal stability of the protein. Superposition of the three dimensional structures of native and mutant luciferases revealed a clear conformational change in the flexible loop between 350–365 in red emitter mutants (Fig. 10A and C) while this conformational change was not observed in mutants with green bioluminescence (Fig. 10B). As shown in Fig. 10E, another important loop in bioluminescence color, which has been considered as a solvent gate for the active site, is a connecting loop between residues 223–235[46] but significant changes between mutant and wild-type enzymes were not found.

Enhancing the stability of proteins and enzymes is one of the main goals of protein engineering. The stabilizing factors in the native protein are the secondary and tertiary interactions, such as van der Waals interactions, hydrogen bonds, and salt bridges. In some proteins there are also covalent bonds between cysteine residues, disulfide bridges, which stabilize the structure. One possible way of increasing the global stability is therefore to engineer disulfide bonds into a protein of known structure.[47]

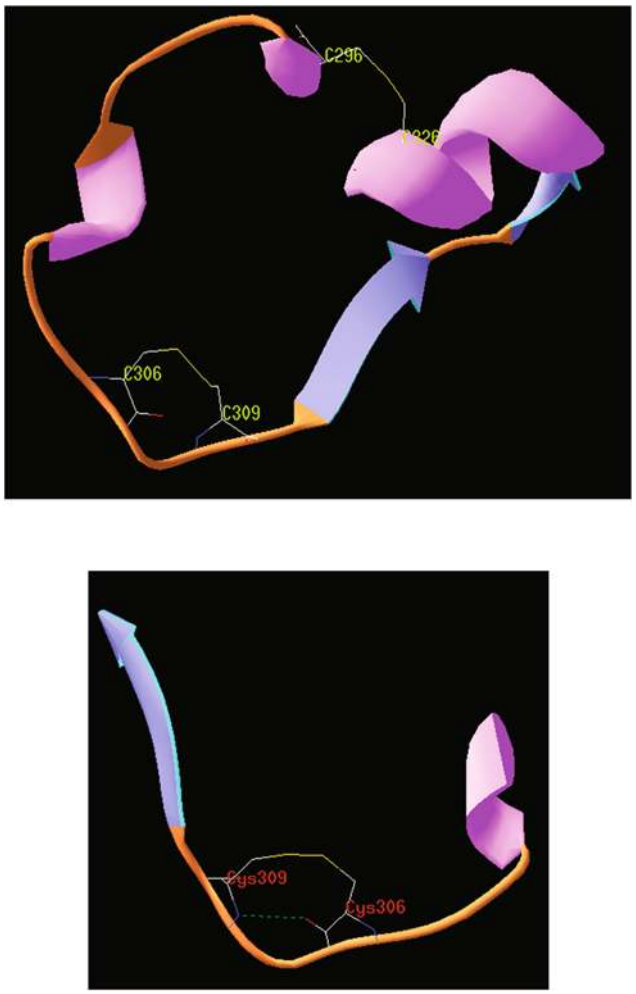


**Fig. 9** A stereo representation of the Leu[306] and Leu[309] position, which are replaced by cysteine and produced a single disulfide bridge that is represented in yellow.

Disulfide bonds stabilize the protein by restraining the unfolded state and thereby reducing the entropy loss upon refolding.[48] When a new disulfide bond is introduced into a protein, the stability rarely increases as much as predicted. This may be due to several factors that must be subtracted from the theoretical value. One reason could be that the replaced amino acids contributed to the protein stabilization. Another reason can be that the cysteines are not optimally placed with respect to each other, which can induce a slight strain in the molecule.[48]

Furthermore, it has been suggested that disulfide bridges increase the free energy of the denatured state by decreasing configurational entropy, thus driving the two state equilibrium (N ↔ D) to the left.[49] Therefore, since we have previously reported the introduction of a disulfide bond in firefly luciferase, which was accompanied by an increase of thermostability, a red shift in color spectra and a decrease of pH-sensitivity.[18,19] In the present work, we have introduced two disulfide bridges in luciferase and characterized the structural stability of firefly luciferase (*P. pyralis*) and its mutants by equilibrium unfolding studies, using urea as a protein denaturant. The free energy of unfolding ($\Delta G_U$) is used as a measure of the stability of the protein to denaturants. $\Delta G(H_2O)$ values for a protein are obtained from analysis of the denaturation curves.[20]

In order to investigate the role of the disulfide bridge in native (*P. pyralis*) and mutant luciferases, color differences and the stability were studied. Insertion of a disulfide bridge in *P. pyralis* luciferase led to increasing of specific activity and decrease of luciferase pH sensitivity.[18]

Indeed, a direct relation between thermostability and color shift to red-region has been observed for mutant luciferases.[10,19,50] Therefore, it was suggested that higher thermostability due to higher luciferase rigidity in protein harboring disulfide bridge(s) could be an alternative mechanism of color shift in firefly luciferase, presumably through more solvent accessibility to the emitter site.[19,51]

In the present work, to investigate the structural changes related to bioluminescence color shift to red and thermal stability, we have carried out structural analysis to determine the effect of these mutations on native and denatured structural states, followed by stability comparison of native (*P. pyralis*) and mutant ($C^{81}$–$A^{105}C$, $L^{306}C$–$L^{309}C$, $P^{451}C$–$V^{469}C$, $C^{81}$–$A^{105}C$/$P^{451}C$–$V^{469}C$, and $A^{296}C$–$A^{326}C$/$P^{451}C$–$V^{469}C$) luciferases by spectroscopic methods.

To understand the effect of additional residues on chemical stability, purified native and mutant luciferases were compared by fluorescence spectroscopy. As indicated in Fig. S6,† the fluorescence intensity of native luciferase was decreased at different concentrations of urea. The reduction of fluorescence suggested that tryptophans ($Trp^{417}$, $Trp^{426}$) are entirely exposed to the solvent due to denaturation of the enzyme, which itself leads to conformational changes.

As indicated in Fig. S6† the presence of an additional disulfide bond increased structural stability of the mutant luciferases compared to the native form. Among the disulfide bonds, $L^{306}C$–$L^{309}C$ has been added in a region containing a flexible loop $K^{303}$YDCSNCH$^{310}$ (Fig. 9). The behavior of this mutant in 0.0–2.0 M urea was very different, the increase of fluorescence resulting from the compacting structure of this mutant. In addition, ANS binding was studied at all concentrations of urea. Considering the extrinsic fluorescence of ANS, intensity increased in native luciferase, but ANS fluorescence emission in other mutants did not show any remarkable change with different concentrations of urea. Upon exposure of hydrophobic clusters or pockets during the unfolding process, ANS binds to proteins.[39] Hence, less binding of ANS to mutants ($C^{81}$–$A^{105}C$, $L^{306}C$–$L^{309}C$, and $P^{451}C$–$V^{469}C$) under denaturation conditions, indicates lower exposure of such regions during chemical denaturation (Fig. 6). After incubation of the enzyme and determination of $\Delta G_{H2O}$ and $D_{1/2}$ (described in the Materials and methods section), it was observed that mutants were more stable than the native enzyme. Thus, $\Delta G_{H2O}$ values of native and mutant luciferases upon urea denaturation are significantly different (Table 2). Comparison of structural stability of native and mutant luciferases revealed the important role of flexible loops in the structural stability of

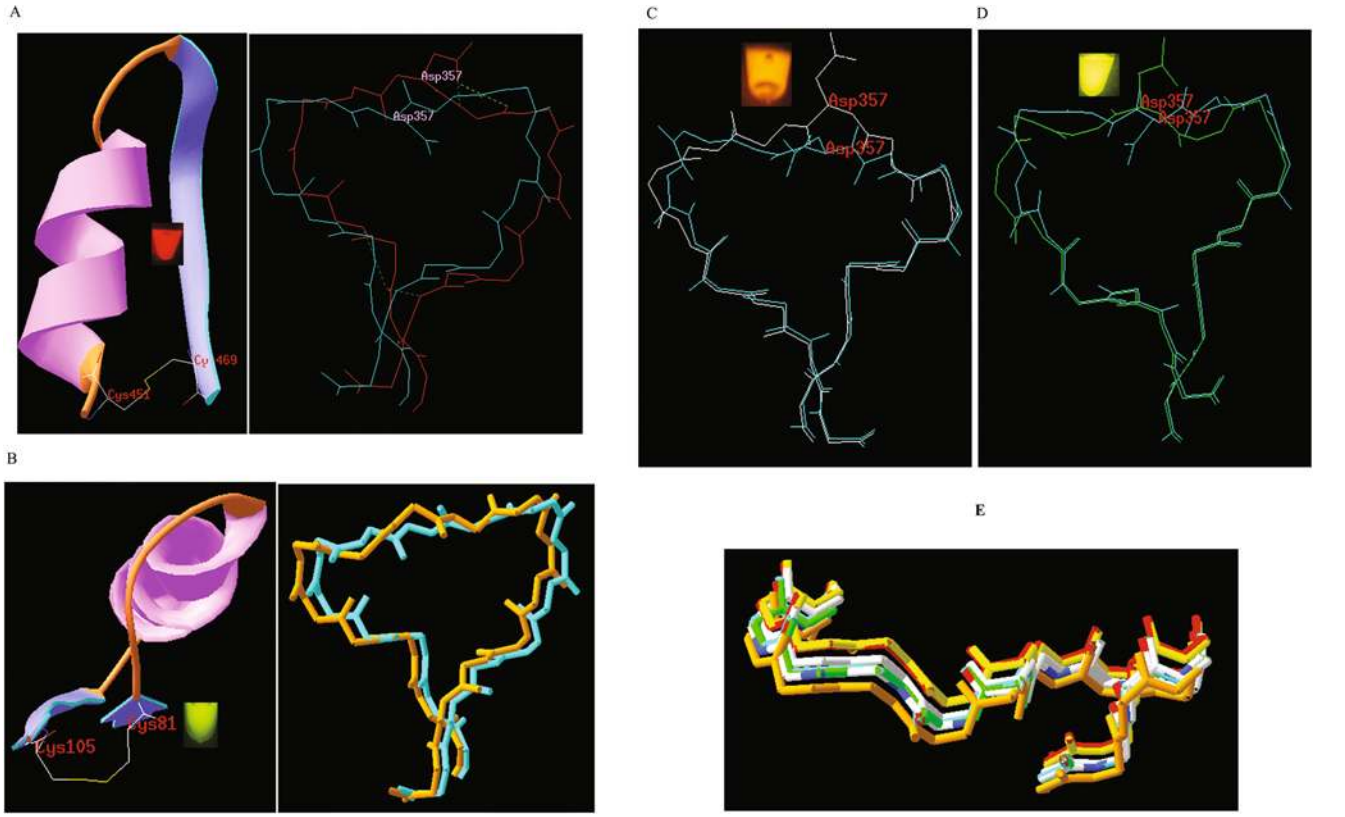


**Fig. 10** Superposition of flexible loop (residues 350–365) models in (A) wild-type (blue) and mutant $P^{451}C$–$V^{469}C$ (red), (B) $C^{81}$–$A^{105}C$ (orange), (C) $A^{296}C$–$A^{326}C$/$P^{451}C$–$V^{469}C$ (white) and D) $C^{81}$–$A^{105}C$/$P^{451}C$–$V^{469}C$ (green) luciferases. The insertion of a disulfide bridge yields displacement of the flexible loop in comparison with that of the wild-type luciferase.

firefly luciferase (Fig. 5A, B). Also, the activity measurements in different urea concentrations showed higher stability of mutants than the native protein. That is to say, higher thermal stabilities of mutant firefly luciferases (Table 1) were also confirmed by measurement of residual activity in the presence of different concentrations of urea. Increase in residual activity in 0.0–1.5 M urea in $L^{306}C$–$L^{309}C$ mutants (Fig. 7) confirmed that the increase in fluorescence emission was not as a consequence of quenching, we have also determined the specific activity of this mutant in the presence of different concentrations of urea, and its specific activity was also increased 2 times in the 0.0–1.5 M urea, whilst it was reduced in native and the other mutants.

Therefore, we can conclude that the insertion of a disulfide bridge leads to more stability (as discussed earlier). Structural stabilities in mutant luciferases were confirmed by spectroscopic studies. This shows that changes in a distant area cause long-range interactions, which in turn could modify the structure of the luciferase active site; and alter the color of the emitted light, similar to some other luciferase mutants.[32] However, mutagenesis in the most flexible region of firefly luciferase confirmed a direct relationship between stability and flexibility in firefly luciferases.[52] In conclusion, native and mutant luciferases followed a two state F ↔ U unfolding mechanism during urea denaturation. The $\Delta(\Delta G)$ of mutant luciferases ($C^{81}$–$A^{105}C$, $L^{306}C$–$L^{309}C$, $P^{451}C$–$V^{469}C$, $C^{81}$–$A^{105}C$/$P^{451}C$–$V^{469}C$, and $A^{296}C$–$A^{326}C$/$P^{451}C$–$V^{469}C$) suggests that the rigidity of the flexible loop significantly contributes to the enzyme's conformational stability. Accordingly, amongst all types of luciferases, the key luciferase residues at the luciferin binding site are entirely conserved. We suggest here that higher free energy of unfolding ($\Delta G_{H2O}$) for $L^{306}C$–$L^{309}C$ mutant (compared to native luciferase) would be responsible for the stability and emission at higher wavelengths (red emission). This investigation may explain the role of flexible loops in the structure of the firefly luciferase superfamily, since the $P^{451}C$–$V^{469}C$ mutant had more energy (1.25 kJ $mol^{-1}$ $\Delta G_{H2O}$) compared to $C^{81}$–$A^{105}C$. It may be suggested that the addition of a disulfide bridge and rigidity in the C-terminal domain of *Ppy* had more effect on the structural stability than the N-terminal domain of the protein.

A comparative study among functional flexible loops of firefly luciferase structure emphasizes the implication of an important flexible loop (352–359) in the control of color emission in red-emitter firefly luciferases (Fig. 10). As is obvious from this model, the introduction of a disulfide bridge brought about displacement of the flexible loop in red-emitters while in the other mutants with green emission such displacements were not observed (Fig. 10). This observation is very similar to those reported mutants with a single amino acid insertion in the same flexible loop.[36] Another related observation for displacement of the flexible loop in the red mutant

 

is the change in the hydrogen bond networks of $Asp^{356}$, $Asp^{357}$ and $Lys^{358}$. In the crystal structure of the native form the hydrogen bond between $Lys^{358}$ (N) and $Asp^{357}$ (OD1) was observed. Moreover, two strong hydrogen bonds between $Lys^{358}$N and $Asp^{357}$ (OD1) and $Asp^{357}$N and $Asp^{356}$ (OD1) were observed within the distance range of 2.6–3.2 Å in the $P^{451}C$–$V^{469}C$ mutant. However, the last hydrogen bond was not observed in the native form and therefore it may be suggested that the change in the H-bond network may displace the flexible loop (Fig. S7A and B†).

Therefore, introduction of a disulfide bridge in a far location compared to the flexible loop induces conformational displacement in the mentioned loop, presumably through long-range interactions and thereby makes the emitter site (oxyluciferin) more solvent accessible.

## Acknowledgements

This work was supported by a grant from the Iranian National Science Foundation (INSF) and Research Council of Tarbiat Modares University.

## References

1 L. F. Greer III and A. A. Szalay, Imaging of light emission from the expression of luciferases in living cells and organisms: a review, *Luminescence*, 2002, **17**, 43–74.
2 J. Hastings, Chemistries and colors of bioluminescent reactions: a review, *Gene*, 1996, **173**, 5–11.
3 A. B. Lall, D. S. F. Ventura, E. J. H. Bechara, J. M. de Souza, P. Colepicolo-Neto and V. R. Viviani, Spectral correspondence between visual spectral sensitivity and bioluminescence emission spectra in the click beetle pyrophorus punctatissimus (coleoptera: elateridae), *J. Insect Physiol.*, 2000, **46**, 1137–1141.
4 R. E. Schmitter, D. Njus, F. M. Sulzman, V. D. Gooch and J. Hastings, Dinoflagellate bioluminescence: a comparative study of *in vitro* components, *J. Cell. Physiol.*, 1976, **87**, 123–134.
5 V. Viviani, The origin, diversity, and structure function relationships of insect luciferases, *Cell. Mol. Life Sci.*, 2002, **59**, 1833–1850.
6 V. Viviani, A. Silva, G. Perez, R. Santelli, E. Bechara and F. Reinach, Cloning and molecular characterization of the cDNA for the Brazilian larval click-beetle pyrearinus termitilluminans luciferase, *Photochem. Photobiol.*, 1999, **70**, 254–260.
7 M. Deluca and W. McElroy, Purification and properties of firefly luciferase, *Methods Enzymol.*, 1978, **57**, 3–15.
8 Y. Ando, K. Niwa, N. Yamada, T. Enomoto, T. Irie, H. Kubota, Y. Ohmiya and H. Akiyama, Firefly bioluminescence quantum yield and colour change by pH-sensitive green emission, *Nat. Photonics*, 2007, **2**, 44–47.
9 H. Seliger and W. McElroy, Spectral emission and quantum yield of firefly bioluminescence, *Proc. Natl. Acad. Sci. U. S. A.*, 1960, **88**, 136–141.
10 B. S. Alipour, S. Hosseinkhani, S. K. Ardestani and A. Moradi, The effective role of positive charge saturation in bioluminescence color and thermostability of firefly luciferase, *Photochem. Photobiol. Sci.*, 2009, **8**, 847–855.
11 B. R. Branchini, D. M. Ablamsky, M. H. Murtiashaw, L. Uzasci, H. Fraga and T. L. Southworth, Thermostable red and green light-producing firefly luciferase mutants for bioluminescent reporter applications, *Anal. Biochem.*, 2007, **361**, 253–262.
12 G. H. E. Law, O. A. Gandelman, L. C. Tisi, C. R. Lowe and J. A. H. Murray, Mutagenesis of solvent-exposed amino acids in *Photinus pyralis* luciferase improves thermostability and pH-tolerance, *Biochem. J.*, 2006, **397**, 305–312.
13 A. Riahi-Madvar and S. Hosseinkhani, Design and characterization of novel trypsin-resistant firefly luciferases by site-directed mutagenesis, *Protein Eng., Des. Sel.*, 2009, **22**, 655–663.
14 L. Tisi, P. White, D. Squirrell, M. Murphy, C. Lowe and J. Murray, Development of a thermostable firefly luciferase, *Anal. Chim. Acta*, 2002, **457**, 115–123.
15 P. J. White, D. J. Squirrell, P. Arnaud, C. R. Lowe and J. Murray, Improved thermostability of the North American firefly luciferase: saturation mutagenesis at position 354, *Biochem. J.*, 1996, **319**, 343–350.
16 K. Hirokawa, N. Kajiyama and S. Murakami, Improved practical usefulness of firefly luciferase by gene chimerization and random mutagenesis, *Biochim. Biophys. Acta, Protein Struct. Mol. Enzymol.*, 2002, **1597**, 271–279.
17 A. Roda, *Bioluminescence and Chemiluminescence: Perspectives for the 21st Century: Proceedings of the 10th International Symposium on Bioluminescence and Chemiluminescence Held at Bologna, Italy, September, 1998*, John Wiley, 1999.
18 M. Imani, S. Hosseinkhani, S. Ahmadian and M. Nazari, Design and introduction of a disulfide bridge in firefly luciferase: increase of thermostability and decrease of pH sensitivity, *Photochem. Photobiol. Sci.*, 2010, **9**, 1167–1177.
19 M. Nazari and S. Hosseinkhani, Design of disulfide bridge as analternative mechanism for color shift in firefly luciferase and development of secreted luciferase, *Photochem. Photobiol. Sci.*, 2011, **10**, 1203–1215.
20 C. N. Pace, D. V. Laurents and J. A. Thomson, pH Dependence of the urea and guanidine hydrochloride denaturation of ribonuclease A and ribonuclease T1, *Biochemistry*, 1990, **29**, 2564–2572.
21 C. Pace and J. Hermans, The stability of globular protein, *Crit. Rev. Biochem. Mol. Biol.*, 1975, **3**, 1–43.
22 P. L. Privalov and S. J. Gill, Stability of protein structure and hydrophobic interaction, *Adv. Protein Chem.*, 1988, **39**, 191.
23 W. M. Jackson and J. F. Brandts, Thermodynamics of protein denaturation. Calorimetric study of the reversible denaturation of chymotrypsinogen and conclusions

regarding the accuracy of the two-state approximation, *Biochemistry*, 1970, **9**, 2294–2301.
24 P. Privalov and N. Khechinashvili, A thermodynamic approach to the problem of stabilization of globular protein structure: a calorimetric study, *J. Mol. Biol.*, 1974, **86**, 665–684.
25 P. L. Privalov and S. A. Potekhin, Scanning microcalorimetry in studying temperature-induced changes in proteins, *Methods Enzymol.*, 1986, **131**, 4–51.
26 R. F. Greene and C. N. Pace, Urea and guanidine hydrochloride denaturation of ribonuclease, lysozyme, α-chymotrypsin, and β-lactoglobulin, *J. Biol. Chem.*, 1974, **249**, 5388–5393.
27 C. Pace, Determination and analysis of urea and guanidine hydrochloride denaturation curves, *Methods Enzymol.*, 1986, **131**, 266–280.
28 M. M. Santoro and D. Bolen, Unfolding free energy changes determined by the linear extrapolation method. 1. Unfolding of phenylmethanesulfonyl. alpha.-chymotrypsin using different denaturants, *Biochemistry*, 1988, **27**, 8063–8068.
29 M. M. Santoro and D. Bolen, A test of the linear extrapolation of unfolding free energy changes over an extended denaturant concentration range, *Biochemistry*, 1992, **31**, 4901–4907.
30 B. W. Matthews, Studies on protein stability with T4 lysozyme, *Adv. Protein. Chem.*, 1995, **46**, 249–278.
31 D. Shortle, Probing the determinants of protein folding and stability with amino acid substitutions, *J. Biol. Chem.*, 1989, **264**, 5315–5318.
32 S. Hosseinkhani, Molecular enigma of multicolor bioluminescence of firefly luciferase, *Cell. Mol. Life Sci.*, 2011, **68**, 1167–1182.
33 K. Khalifeh and B. S. Alipour, The effect of surface charge balance on thermodynamic stability and kinetics of refolding of firefly luciferase, *BMB Rep.*, 2011, **44**, 102–106.
34 N. Tafreshi, M. Sadeghizadeh, R. Emamzadeh, B. Ranjbar, H. Naderi-Manesh and S. Hosseinkhani, Site-directed mutagenesis of firefly luciferase: implication of conserved residue (s) in bioluminescence emission spectra among firefly luciferases, *Biochem. J.*, 2008, **412**, 27–33.
35 P. Maghami, B. Ranjbar, S. Hosseinkhani, A. Ghasemi, A. Moradi and P. Gill, Relationship between stability and bioluminescence color of firefly luciferase, *Photochem. Photobiol. Sci.*, 2010, **9**, 376–383.
36 A. Moradi, S. Hosseinkhani, H. Naderi-Manesh, M. Sadeghizadeh and B. S. Alipour, Effect of charge distribution in a flexible loop on the bioluminescence color of firefly luciferases, *Biochemistry*, 2009, **48**, 575–582.
37 M. Mortazavi and S. Hosseinkhani, Design of thermostable luciferases through arginine saturation in solvent-exposed loops, *Protein Eng., Des. Sel.*, 2011, **24**, 893–903.
38 C. A. Royer, Approaches to teaching fluorescence spectroscopy, *Biophys. J.*, 1995, **68**, 1191.
39 G. Semisotnov, N. Rodionova, O. Razgulyaev, V. Uversky, A. Gripas and R. Gilmanshin, Study of the "molten globule" intermediate state in protein folding by a hydrophobic fluorescent probe, *Biopolymers*, 1991, **31**, 119–128.
40 C. N. Pace and J. M. Scholtz, Measuring the conformational stability of a protein, *Protein Struct.: A Practical Approach*, 1997, **2**, 299–321.
41 N. Fernandez-Fuentes, C. J. Madrid-Aliste, B. K. Rai, J. E. Fajardo and A. Fiser, M4T: a comparative protein structure modeling server, *Nucleic Acids Res.*, 2007, **35**, W363–W368.
42 D. Rykunov, E. Steinberger, C. J. Madrid-Aliste and A. Fiser, Improved scoring function for comparative modeling using the M4T method, *J. Struct. Funct. Genomics*, 2009, **10**, 95–99.
43 K. Tina, R. Bhadra and N. Srinivasan, PIC: protein interactions calculator, *Nucleic Acids Res.*, 2007, **35**, W473–W476.
44 G. L. Ellman, Tissue sulfhydryl groups, *Arch. Biochem. Biophys.*, 1959, **82**, 70–77.
45 H. Fraga, Firefly luminescence: a historical perspective and recent developments, *Photochem. Photobiol. Sci.*, 2008, **7**, 146–158.
46 V. R. Viviani, A. J. Silva Neto, F. G. C. Arnoldi, J. A. R. G. Barbosa and Y. Ohmiya, The influence of the loop between residues 223–235 in beetle luciferase bioluminescence spectra: a solvent gate for the active site of pH-sensitive luciferases, *Photochem. Photobiol.*, 2008, **84**, 138–144.
47 M. Matsumura and B. W. Matthews, Stabilization of functional proteins by introduction of multiple disulfide bonds, *Methods Enzymol.*, 1991, **202**, 336–356.
48 M. Matsumura, W. J. Becktel, M. Levitt and B. W. Matthews, Stabilization of phage T4 lysozyme by engineered disulfide bonds, *Proc. Natl. Acad. Sci. U. S. A.*, 1989, **86**, 6562–5666.
49 J. M. Mason, M. J. Cliff, R. B. Sessions and A. R. Clarke, Low energy pathways and non-native interactions, *J. Biol. Chem.*, 2005, **280**, 40494–40499.
50 S. F. Betz, Disulfide bonds and the stability of globular proteins, *Protein Sci.*, 1993, **2**, 1551–1558.
51 R. A. Deshpande, M. I. Khan and V. Shankar, Equilibrium unfolding of RNase Rs from Rhizopus stolonifer: pH dependence of chemical and thermal denaturation, *Biochim. Biophys. Acta, Proteins Proteomics*, 2003, **1648**, 184–194.
52 Z. A. Bayat, S. Hosseinkhani, R. Jafari and K. Khajeh, Relationship between stability and flexibility in the most flexible region of *Photinus pyralis* luciferase, *Biochim. Biophys. Acta, Proteins Proteomics*, 2011, **1824**, 350–358.

 